

MILCA: A Maximum Internal Linear Component Analysis for the extraction of spectral emissions.

G. Hurier, S. R. Hildebrandt, J. F. Macías-Pérez

Laboratoire de physique subatomique et de cosmologie, Grenoble

Received <date> / Accepted <date>

Abstract

The present work deals with the problem of extracting a sky map of a particular emission process that has been observed in an experiment with different detectors each of them having a different spectral response. This is the arena of the so-called “methods of component separation”, especially in the field of microwave experiments, like the Cosmic Background Microwave (CMB) missions COBE, WMAP or, at present, the Planck surveyor mission. For the Internal Linear Combination methods, the difference with respect to other approaches is that it uses only the spectral behaviour of the sought component as an input. This idea has been applied to the case of CMB emission. Since this emission is itself the calibration emission in those maps, the problem is simplified. In this work, we derive the general expression for a generic spectral behaviour of the sought emission. We also apply the method to some of the common missions in the range of microwave and sub-mm emissions: Galactic dust, Synchrotron emission, Sunyaev-Zel’dovich effect and as a check for consistency to CMB also. The data are simulations that resemble those performed presently by the Planck surveyor mission. Moreover, we will also show how it is possible to optimize the extraction of the chosen emission by minimizing the output noise and the bias in the extraction of the component. Therefore, we call this method MILCA: Maximum Internal Linear Component Analysis.

Key words. cosmic microwave background – Component separation – Data analysis

1. Introduction

The Planck space mission (The PLANCK collaboration) was launched on the 14th May 2009, is the third space mission, after the COBE (19; 2) and the WMAP (11; 12; 3). The Planck mission is a typical CMB experiment, where the sky is observed at different frequencies. The Planck mission is observing the whole sky at 9 frequency channels, 3 of them at 30 GHz, 44 GHz and 70 GHz constitute the so-called Low Frequency Instrument, LFI, and the other 6 channels, at 100 GHz, 143 GHz, 217 GHz, 353 GHz, 545 GHz and 857 GHz, constitute the so-called High Frequency Instrument, HFI.

In the following, we will write the value of the emission of a all sky map as:

$$\mathbf{T} = \mathbf{A} \cdot \mathbf{S} + \mathbf{N} \quad (1)$$

where \mathbf{T} is vector containing all the observations at the different channels, \mathbf{A} is a matrix, called “the mixing matrix”. It has dimensions of $n_t \times n_s$, where n_t is the number of detectors, or elements in the vector \mathbf{T} , and n_s is the number of components, or elements in the vector \mathbf{S} . \mathbf{S} is a vector whose components are the values of the component to be extracted at each of the detectors and \mathbf{N} is the noise contribution. We use the notation $\mathbf{A} \cdot \mathbf{B}$ to denote the usual matrix product.

In other component separation techniques, such as Maximum Likelihood techniques (8) or Maximum of

Entropy method (15; 16) one uses a priori knowledge about the component term and/or mixing matrix \mathbf{A} . On the other hand, the ILC technique (3) assumes a limited knowledge on the mixing matrix \mathbf{A} : only one component have a known spectrum. In the usual case of the CMB emission, one readily has that the spectrum of the source is flat, simply due to the fact that the data are calibrated with respect to the CMB itself. Finally techniques like the Independent Component Analysis ICA (14; 4; 5), renders the matrix \mathbf{A} as an unknown.

We will show in this paper, step by step from ILC to MILCA, that it is possible to minimize the effect of the bias and noise by imposing additional conditions in the determination of the wanted component. The same idea is valid both for the case of a diffuse emission or a point-source one.

2. Generalisation of ILC for a non-flat spectrum emission: the noiseless case

In this section, we assume that there is no noise term in the map-making or it can be disregarded at a first approximation and let for the next one the case with the addition of noise. Then, one has

$$\mathbf{T} = \mathbf{A} \cdot \mathbf{S}, \quad (2)$$

where, we remind that \mathbf{T} is a vector containing the observed values for each of the channels. \mathbf{A} is the so-called

mixing matrix and contains the frequency dependence of the different physical components. It is defined as:

$$A_{ij} = \int F_i(\nu) H_j(\nu) d\nu \quad (3)$$

where $F_i(\nu)$ is the frequency dependence of the i -th component and $H_j(\nu)$ is the spectral response of the detector j . \mathbf{T} is the vector containing the observed values in the map for each of the channels. Finally, \mathbf{S} is the vector containing each template map of the physical effects and for the different observed frequencies (channels).

2.1. Method

Let us consider

$$S_c = \sum_i w_i T_i \quad (4)$$

$$S_c = \mathbf{w}^T \cdot \mathbf{T}, \quad (5)$$

where S_c is the component we want to extract. The vector \mathbf{w} contains the set of weights that will be used to obtain that particular component by *linear combination*. Now we will describe how \mathbf{w} is determined.

In order to obtain \mathbf{w} , we proceed as in the well-known ILC method for CMB emission but allow for a non-flat spectrum in the emission law of the component to be extracted. That is, \mathbf{w} will be determined by minimizing the variance under the following constraint

$$g = \sum_i f_i w_i = 1, \quad (6)$$

where \mathbf{f} is a vector containing the frequency dependence of the component to be extracted at each channel. The vector \mathbf{f} is related to \mathbf{A} by $\mathbf{f} = \mathbf{e}_c^T \cdot \mathbf{A}$, where \mathbf{e}_c is a column vector whose values are 0 except for the " c "-th entry, associated to the component to extract, for which its value is 1.

The variance to be minimized is given by

$$V(S_c) = \mathbf{w}^T \cdot \mathbf{T} \cdot \mathbf{T}^T \cdot \mathbf{w}, \quad (7)$$

where $V(S_c)$ is the variance of the component extracted by a linear combination of observed channels. We solve Eq. (7) by using Lagrange multipliers

$$\nabla V(S_c) - \lambda \cdot \nabla g = 0, \quad (8)$$

$$g = 1, \quad (9)$$

where λ is some constant.

The gradient of $V(S_c)$ and g are given by

$$\nabla V(S_c) = 2 \cdot \mathbf{C}_T \cdot \mathbf{w}, \quad (10)$$

$$\nabla g = \mathbf{f}, \quad (11)$$

where \mathbf{C}_T is the covariance matrix of the observed map. Eq. (9) can be expressed in matricial notation

$$\begin{pmatrix} 2 \cdot \mathbf{C}_T & -\mathbf{f} \\ \mathbf{f}^T & 0 \end{pmatrix} \begin{pmatrix} \mathbf{w} \\ \lambda \end{pmatrix} = \begin{pmatrix} \mathbf{0} \\ 1 \end{pmatrix} \quad (12)$$

This system of equations can be solved by using a block inversion method, whose general expression can be written as

$$\mathbf{M} = \begin{pmatrix} \mathbf{A} & \mathbf{B} \\ \mathbf{C} & \mathbf{D} \end{pmatrix}, \quad (13)$$

$$\mathbf{M}^{-1} = \begin{pmatrix} \mathbf{A}^{-1} + \mathbf{A}^{-1} \cdot \mathbf{B} \cdot (\mathbf{D} - \mathbf{C} \cdot \mathbf{A}^{-1} \cdot \mathbf{B})^{-1} \cdot \mathbf{C} \cdot \mathbf{A}^{-1} & -\mathbf{A}^{-1} \cdot \mathbf{B} \cdot (\mathbf{D} - \mathbf{C} \cdot \mathbf{A}^{-1} \cdot \mathbf{B})^{-1} \\ -(\mathbf{D} - \mathbf{C} \cdot \mathbf{A}^{-1} \cdot \mathbf{B})^{-1} \cdot \mathbf{C} \cdot \mathbf{A}^{-1} & (\mathbf{D} - \mathbf{C} \cdot \mathbf{A}^{-1} \cdot \mathbf{B})^{-1} \end{pmatrix}$$

With this in hand, the result for the \mathbf{w} estimator is given by

$$\widehat{\mathbf{w}} = \frac{\widehat{\mathbf{C}}_T^{-1} \cdot \mathbf{f}}{\mathbf{f}^T \cdot \widehat{\mathbf{C}}_T^{-1} \cdot \mathbf{f}} \quad (14)$$

The same results has been obtain in parallel by (17).

One can readily see that for a flat spectrum, as it is the case of the CMB emission, we obtain the same results as the well-known ILC method Eq.15 given by (7), i.e.

$$\widehat{\mathbf{w}} = \frac{\widehat{\mathbf{C}}_T^{-1} \cdot \mathbf{1}}{\mathbf{1}^T \cdot \widehat{\mathbf{C}}_T^{-1} \cdot \mathbf{1}} \quad (15)$$

From Eq. (14) we can derive the estimator of S_c which is given by

$$\widehat{S}_c = \frac{\mathbf{f}^T \cdot \widehat{\mathbf{C}}_T^{-1} \cdot \mathbf{T}}{\mathbf{f}^T \cdot \widehat{\mathbf{C}}_T^{-1} \cdot \mathbf{f}} \quad (16)$$

2.2. Properties of the noiseless estimator

In this section, we develop the explicit expression of Eq. (16) for the case of Eq. (2). For this case, we obtain

$$\mathbf{C}_T = \mathbf{A} \cdot \mathbf{C}_S \cdot \mathbf{A}^T, \quad (17)$$

where \mathbf{C}_S is the covariance matrix associated to each component.

Some precaution must be taken before inverting \mathbf{C}_T . This matrix has dimension $n_t \times n_t$ but has rank $\min(n_s, n_t)$ by construction.

There are three possible cases.

- The case $n_s > n_t$: we have a lower number of detectors than the number of components. In this case, it is not guaranteed that a linear combination can provide an isolation of the wanted component. Indeed, in this situation the ILC method is not efficient and can provide severe bias.
- The case $n_s = n_t$: we have the same number of detectors and physical components. In this case \mathbf{A} is a square matrix, so there is no ambiguity when inverting \mathbf{C}_T . The procedure is straightforward.
- The case $n_s < n_t$: in this case \mathbf{C}_T has rank $n_s < n_t$. Consequently, the matrix is singular and can not be inverted. However, one may take its pseudo-inverse as defined from well-known singular value decomposition (SVD) defined as $\mathbf{C}_T^{-1} = \mathbf{U} \cdot \mathbf{D}^{-1} \cdot \mathbf{U}^T$, where \mathbf{D} is a diagonal matrix containing the singular values of \mathbf{C}_T and \mathbf{U} is an orthogonal matrix obtained from singular value decomposition of \mathbf{C}_T . With this in hanf, one can write $\mathbf{C}_T = \mathbf{U} \cdot \mathbf{D} \cdot \mathbf{U}^T$. We remark

that in this case \mathbf{D} is uniquely defined, but \mathbf{U} is not and has still $n_t - n_s$ degrees of freedom showing the fact that there are indeed multiple linear combinations of \mathbf{T} elements which extract the wanted component.

In the sequel, we will only consider the cases $n_s \leq n_t$. The results we obtain for the S_c estimator is given by

$$\widehat{S}_c = \frac{\mathbf{1}^T \cdot (\mathbf{A} \cdot \widehat{\mathbf{C}}_S \cdot \mathbf{A}^T)^{-1} \cdot \mathbf{A} \cdot \mathbf{S}}{\alpha} \quad (18)$$

$$\alpha = \mathbf{f}^T \cdot \widehat{\mathbf{C}}_T^{-1} \cdot \mathbf{f} \quad (19)$$

$$\mathbf{f} = \mathbf{A} \cdot \mathbf{e}_c \quad (20)$$

$$\mathbf{A}^{-1} \cdot \mathbf{f} = \mathbf{A}^{-1} \cdot \mathbf{A} \cdot \mathbf{e}_c = \mathbf{e}_c \quad (21)$$

$$\alpha = (\widehat{\mathbf{C}}_S^{-1})_{cc} \quad (22)$$

$$\widehat{S}_c = \frac{\mathbf{e}_c^T \cdot (\widehat{\mathbf{C}}_S)^{-1} \cdot \mathbf{S}}{\alpha} \quad (23)$$

$$\widehat{S}_c = S_c + \frac{1}{(\widehat{\mathbf{C}}_S^{-1})_{cc}} \cdot \sum_{j \neq c} (\widehat{\mathbf{C}}_S^{-1})_{cj} \cdot S_j \quad (24)$$

2.3. Application to simulated data

In this section, we apply the expressions obtained so far to the case of dust emission. We do not apply it to other emission laws because we wish to show how the non-inclusion of noise bias the estimator and therefore the previous equations, Eqs. (24), need to be modified to incorporate the noise term, and the case of dust emission has revealed to be the clearer case.

In fig.2 we present the results of extracting a dust component from simulated PLANCK observations at 100 GHz, 143 GHz and 217 GHz with a simulated CMB (using synfast with the best fit of the WMAP 7 years results, see (13)), a dust model (FDS8, (18)) and a synchrotron template (we use Haslam et al. map at 408 MHz (10) in its Healpix form (LAMBDA website)). Each of these templates are shown in Fig.1. In order to simulate the emission at 100 GHz, 143 GHz and 217 GHz, we assume a constant spectral index for the synchrotron of - 3.0 and a grey body at 17 K and with a constant spectral index of + 2.0 for the case of dust. Furthermore, all the maps are finally degraded to the 100 GHz beam of 9.5 arcmin resolution.

In fig.2 we show the importance of the bias due to spacial correlations that is present after applying the noiseless version of the ILC algorithm. Indeed, using a block inversion procedure for \mathbf{C}_S it can be shown that the estimator of S_c is unbiased *only* in the case where the component we want extract is uncorrelated with the other components. This can be shown from Eqs.14. There, one can see that if blocks \mathbf{B} and \mathbf{C} of the matrix are null, the corresponding blocks \mathbf{B} and \mathbf{C} of the inverted matrix will be as well null. Therefore, $(\mathbf{C}_S^{-1})_{cj}$ will be null. If S_c is correlated with some component, a bias will result as shown at eq.24. This bias comes from the fact that the minimum of the variance is not an eigenvector of the component space. In any practical

case \mathbf{C}_S will be correlated foregrounds to some extent (but for the CMB), especially in the Galactic plane. Of course, a simple way to diminish the effect of bias is introducing a mask that would remove most of the regions where correlation is higher, close to the Galactic plane. Yet, we will present in the following question that noise can be included in the algorithm improving the results on the bias.

3. Noise induced bias

Let us remember Eq. (2),

$$\mathbf{T} = \mathbf{A} \cdot \mathbf{S} + \mathbf{N}.$$

The vector \mathbf{N} is a vector containing the noise component for each of the channels. In the noisy case \mathbf{C}_T becomes

$$\mathbf{C}_T = \mathbf{A} \cdot \mathbf{C}_S \cdot \mathbf{A}^T + \mathbf{C}_N, \quad (25)$$

where $\mathbf{C}_N = \mathbf{N} \cdot \mathbf{N}^T$ is the noise covariance matrix.

In this case, the matrix \mathbf{C}_T is invertible. If we further assume as a first hypothesis that instrumental noise among detectors is not correlated at first order \mathbf{C}_N becomes diagonal. Therefore, since \mathbf{C}_N is a n_t rank matrix, so it will be \mathbf{C}_T . However, for $n_s < n_t$ we can no longer describe \mathbf{C}_T within a n_s dimensional subspace. In this situation, the only way would be to increase the dimension of the components space to achieve a dimension equal to the number of detectors. However, in this space \mathbf{C}_S has no longer the physical sense previously defined and will unavoidably produce some extra bias on the S_c estimator. Furthermore, \mathbf{C}_N will contribute to the non diagonal terms in \mathbf{C}_S resulting in a subsequent incrementation of the bias given by

$$\widehat{S}_c = \frac{\mathbf{f}^T \cdot \widehat{\mathbf{C}}_T^{-1} \cdot \mathbf{T}}{\alpha}, \quad (26)$$

$$\alpha = \mathbf{f}^T \cdot \widehat{\mathbf{C}}_T^{-1} \cdot \mathbf{f}, \quad (27)$$

$$\widehat{S}_c = \frac{\mathbf{f}^T \cdot (\mathbf{A} \cdot \widehat{\mathbf{C}}_S \cdot \mathbf{A}^T + \widehat{\mathbf{C}}_N)^{-1} \cdot (\mathbf{A} \cdot \mathbf{S} + \mathbf{N})}{\alpha} \quad (28)$$

In fig.3 we show the bias due to the introduction of noise. The frequency bands are the same as in Fig.2. In this case, the bias remains around 12% of the CMB, which is a huge bias.

In any realistic situation, bias in the estimator can be produced by several different causes. For instance:

- Statistical errors on the estimation of \mathbf{C}_T due to the limited resolution of the experiment.
- Calibration uncertainties that will produce slightly different frequency spectra for the emissions different to the calibration one. This can be translated into an error associated to the mixing matrix \mathbf{A} . Yet, in the case of high signal to noise ratio, ILC is very sensitive to calibration errors as the expected ones in the Planck mission, around 1% (6).
- Difference between true \mathbf{A} and the "a priori" spectrum used for the separation.
- Instrumental noise as we have shown in this section.

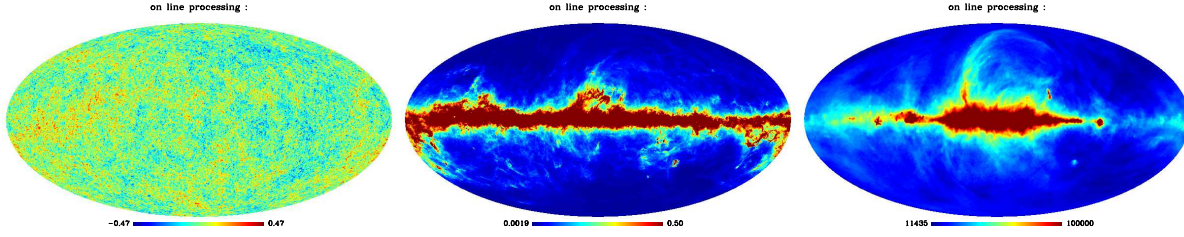


Figure 1. from left to right, simulated CMB whitout noise at a resolution of 9.5 arcmin, dust FDS8 model at 353 GHz and Haslam et al. map for synchrotron at 408 MHz.

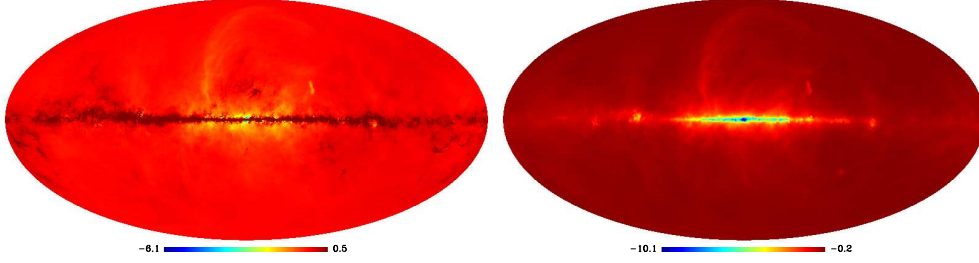


Figure 2. Left : Obtained map with the ILC algorithm for dust whitout noise. It has a total RMS = 0.8. Right : Residual map between the ILC map and the dust input map at 353 GHz showing the bias. The total RMS is now 0.4

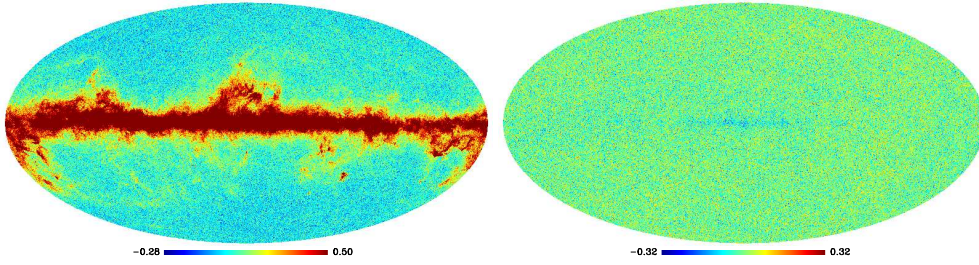


Figure 3. Left: ILC obtained map for dust with noise. The total RMS is 1.02 . Right: bias and noise in the ILC derived map. the total RMS is 0.07, and the RMS of noise is around 0.07

All those effects will contribute to bias on the S_c estimator. We try in the next section to minimize the bias on the estimator.

4. Optimised estimator

The variance associated to the S_c estimator for each pixel is given by eq.30

$$V(p) = \langle S_c(p).S_c(p) \rangle \quad (29)$$

$$V(p) = \frac{f^T \cdot \tilde{C}_T^{-1}}{\alpha} \cdot T(p) \cdot T^T(p) \cdot \frac{\tilde{C}_T^T \cdot f}{\alpha} \quad (30)$$

The error in this technique can be minimized by using the condition number κ which bounds the relative error. Its expression is

$$\widehat{\kappa} = \left\| \frac{\lambda_{max}}{\lambda_{min}} \right\|, \quad (31)$$

where λ_{max} is the maximum eigenvalue of C_T and λ_{min} is the minimal eigenvalue. In a case of low noise and

where $n_s < n_t$, the C_T estimator will be close to a singular matrix (not singular due to the statistic variance associated with the C_T estimation and with instrumental noise), which may result in a severe increase of noise.

4.1. Unbiased estimator

All the issues considered in previous section introduce an additionnal bias on the estimator of S_c . A way to create an unbiased estimator is given by (21).

$$\tilde{C}_T = C_T - C_N \quad (32)$$

Eq.32 provides an unbiased estimator in the case when the covariance matrix of the noise is known and which may be assumed in many practical cases. In this solution \widehat{S}_c is only biased by the correlation between S_c and the other components. The result is the same as obtained in Eq.24. Yet, clearly, one does no longer minimize the variance of noise. This is presented on Fig.4, where we have now use now 2 more frequency bands

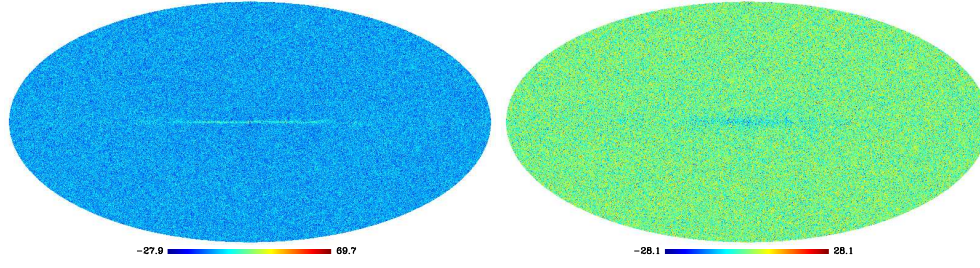


Figure 4. Left: obtained map for dust unbiased estimator using the ILC algorithm. The total RMS is 9.56. Right: Residual map showing the bias. Total RMS is 9.54. The RMS of noise is 9.53

(353 and 545 GHz).

In Fig. 4 we show the result of applying the unbiased estimator. It turns out that when removing the noise, we are close to the case where C_T is nearly singular. And, as expected, there is a severe increase of the noise in the derived ILC map. In fact, there is still a 5% of the CMB emission remaining in those maps.

4.2. Compromise between noise and bias

In the rest of this work we will denote \tilde{C}_T by C_T .

The eigenvalues of C_T which are not too small give us an idea of the number of n_s that may be extracted with a reasonable unbiased and signal to noise.

In the case $n_s < n_t$, the pseudo-inverse of C_T can be defined with $n_t - n_s$ degrees of freedom, as explained in preceding sections. In practice we invert C_T in the subspace of extractible component. Hence, we will use those remaining degrees of freedom for minimizing the noise RMS eq.34. The results obtained for dust are shown in Fig.4. We remark, though, that this technique will introduce some additional bias. In fact any ILC and in particular the present MILCA algorithm will always have to find a compromise between the noise RMS minimisation and the bias removing. In our case, this translates into

$$V_N = \mathbf{w}^T \cdot \mathbf{N} \cdot \mathbf{w} \quad (33)$$

$$\mathbf{g}' = \nabla V_N = 0, \quad (34)$$

where \mathbf{g}' is a new constraint, and \mathbf{w} has only $n_t - n_s$ degrees of freedom. We remember that the minimization of $V(S_c)$ is giving already n_s constraints. In practice, we have minimized \mathbf{g}' using markov chains. We present the obtained MILCA map in fig.5. We obtain a quite well compromise between noise and residual bias.

The Fig.5 shows that the residual bias is however important. Adding some more knowledge about component maps will improve the results as we detail in the next section. Here there is a 9% remaining CMB contribution.

4.3. Improvement by acting on covariance matrix eigenvalues

In the case of an unbiased estimator by removing noise covariance matrix, the eigenvalues of the covariance matrix correspond to the variance associated to the component (in the case where the components are statistically independent from each other). For usual ILC algorithm the component who dominates the signal in the map will have the best efficiency in the ILC procedure. Therefore, by *artificially* increasing an eigenvalue of one of the components, the MILCA algorithm will be minimize this component with a better efficiency.

For instance, we compute the MILCA extraction increasing the eigenvalues associated to all components but dust to have a value 10 time greater than the one associated to dust.

As shown in Fig. 6, we can also use this method to reduce the contribution of a component with an unknown spectrum. In the maps in Fig. 6 the remaining CMB is of 0.34%. This can be very helpful in the case the MILCA component extraction is to be applied in small patches. In this case, one can remove sources with different sort of spectra. This framework will be the matter of the remaining of this paper. We finish this section mentioning that by increasing some of the components, one necessarily degrades the capability of removing the other ones. Therefore, this procedure should not be carried in the case one has a biased estimator, because decreasing the noise would turn into an increase of the noise induced bias.

5. Using additional knowledge of the other components

An additional way to remove the bias is using a "a priori" knowledge about \mathbf{A} , as mentioned in preceding sections. In the case with $n_s < n_t$, one has to use the pseudo inverse of C_T . We define $\tilde{\mathbf{f}}$ as a rectangular matrix (n_t, n_c) with $n_c < n_s$, that will contain the frequency dependence of "a priori" known component. Incidentally, in this way, one also has the possibility of forcing an unwanted component to be null in the final linear combination.

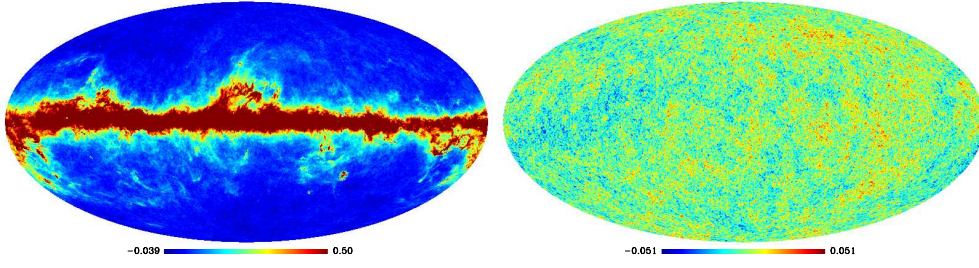


Figure 5. Left: Obtained map with the MILCA algorithm for dust after minimizing for the noise RMS. The total RMS is 1.02. Right: bias in MILCA map. The total RMS is 0.01 and the noise RMS = $4 \cdot 10^{-4}$

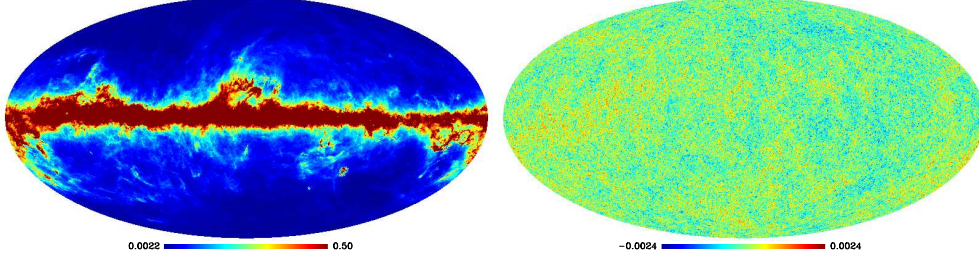


Figure 6. Left: Obtained map using the MILCA algorithm for dust with noise. Total RMS is 1.02. Right: bias and noise from the MILCA map. The corresponding RMS are $5 \cdot 10^{-4}$ and $3 \cdot 10^{-4}$, respectively.

The new system of equations to solve is

$$\nabla V(S_c) - \lambda^T \cdot \nabla g = 0, \quad (35)$$

$$g = \tilde{f}^T \cdot \mathbf{1} = e_1, \quad (36)$$

$$\nabla g = \tilde{f}, \quad (37)$$

with λ a n_c vector of Lagrange multipliers, $\mathbf{1}$ a vector of n_t dimension containing only values 1 and e_1 a n_c dimension vector containing values 1 for the chosen component to be extracted, and 0 for the rest. The new system of equations in matricial notation is

$$\begin{pmatrix} 2 \cdot C_T & -\tilde{f} \\ \tilde{f}^T & \mathbf{0} \end{pmatrix} \begin{pmatrix} w \\ \lambda \end{pmatrix} = \begin{pmatrix} \mathbf{0} \\ e_1 \end{pmatrix} \quad (38)$$

Following the same procedure as in the previous section, we obtain an estimator for S_c given in Eq. 39, with the simple replacement of f by \tilde{f} . Consequently, the properties of this estimator are the same as the ones in the previous section, but have the remarkable advantage of having removed the bias due to the known unwanted component.

$$\widehat{S}_c = \left((\tilde{f}^T \cdot \widehat{C}_T^{-1} \cdot \tilde{f})^{-1} \cdot \tilde{f}^T \cdot \widehat{C}_T^{-1} \right) \cdot T \quad (39)$$

Following a similar idea (adding extra-constrain on ILC like algorithm), an other estimator has been proposed by (17).

Where now subscript c , refers to the " c "-th line of the matrix. The corresponding results are shown in Fig.7. One can see how there is no more a remaining residual from the CMB emission (assuming of course there are

no calibration errors). Clearly, one can also extract other known component by this procedure eq.40.

$$\widehat{S} = (\tilde{f}^T \cdot \widehat{C}_T^{-1} \cdot \tilde{f})^{-1} \cdot \tilde{f}^T \cdot \widehat{C}_T^{-1} \cdot T \quad (40)$$

6. The case of the patches approach.

Application to the thermal SZ recovery

In the preceding sections we have demonstrated that the MILCA method gives good results when applied to a all sky map to recover diffuse emissions. The case of recovering sources can be indeed improved by using the MILCA algorithm in small patches around the source, which is a natural and easy to implement option, once the source candidates are known from some catalogue or method (as e.g. SExtractor (Bertin et al.)).

In fact, this is the only left to proceed since the spectra of the sources covers many different values and the number of components to extract cannot exceed the number of detectors.

Instead of showing how the MILCA algorithm works for some sort of predefined sources with some known spectrum (as e.g., supernova remnants, Gigahertz peaked sources, dusty galaxies, ...) we will apply it to the more common interest case in CMB studies of the thermal-SZ emission.

To that end, we have performed a all-sky simulation, and have modified the thermal dust emission so that when selecting different patches we will also test the methods against variable dust index (between 1.4 and 2.0 smooth at a resolution of 3 degrees) over the sky.

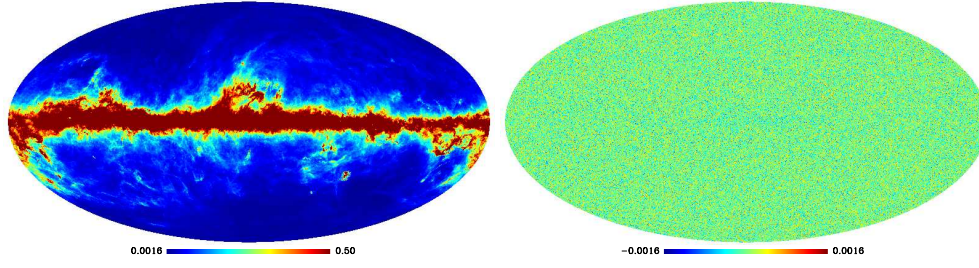


Figure 7. Left: Obtained map with the MILCA algorithm for dust with a suppression of CMB emission. The total RMS is 1.02. Right: bias in MILCA map. The RMS is 3.10^{-4} and the noise RMS is 3.10^{-4} .

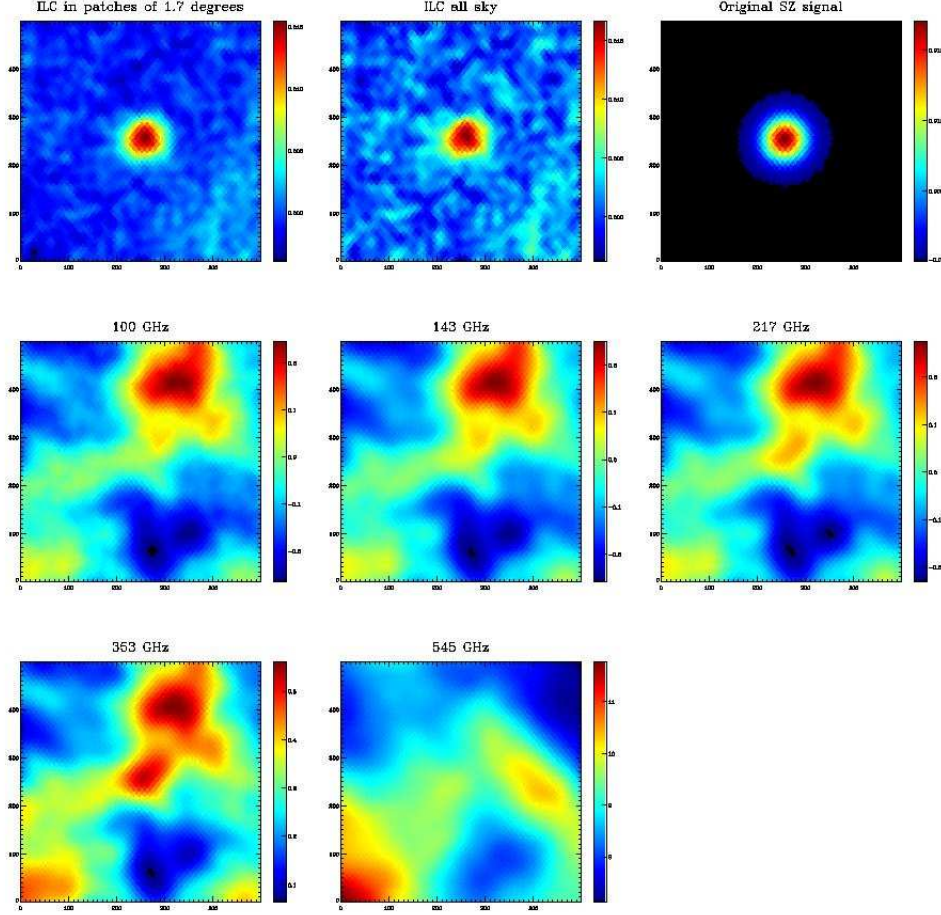


Figure 8. Top: from left to right the map computed with the MILCA algorithm in a patch with a size of 1.7 degrees, the all sky MILCA map and the original signal. Bottom: the different observations at each channel for the 5 HFI frequency bands

In Fig. 8 we present the results of the extraction of the SZ signal for two different cases: if one applies the method to the whole sky and when applied on 1.7 degrees square patches. We obtain lower noise results for the case of the 1.7 degrees square patches. The reason is again in the fact of the available number of independent observations (detectors) and the effective number of components. In the case of real thermal dust emission, the dust component cannot be described by only one spatially constant spectrum, which results in an im-

possibility for any global linear algorithm to remove dust on the whole sky at once. However, as it is clear, when considering smaller regions, as the 1.7 degrees patches the dust spectral index will be in many cases practically constant and the algorithm will provide a better removal of this component.

On the other hand, we remark that the small patches approach has obviously the drawback that the uncertainty of the covariance matrix estimation will be higher, and can yield to some artificial correlation be-

tween an uncorrelated component such as dust, CMB and thermal SZ. So, finally, one should find a compromise between the size of the patch and the limited number of spectra that can be removed by an ILC like algorithm, as the MILCA algorithm is. Nevertheless, let us mention again, that we have provided the tools and the main ideas to be applied to each particular, real, situation.

7. Conclusion

We have presented a method for extracting a chosen component from a map which is the result of the contributions of different components, as is the usual situation in the area of microwave and submm observations, like all CMB experiments.

In a first step, we have used our knowledge on the frequency dependence on n_c known component for constraining the weights that allow to extract that component from the mixture by an, internal, linear combination.

In a second step, we minimize the variance of the chosen component obtaining $n_s - n_c$ constraints on the weight of MILCA.

Finally, we use the last $n_t - n_s$ degrees of freedom for minimizing the noise covariance matrix.

As a result, we have shown how we obtain a good compromise between bias removal and noise RMS minimization.

As for improving the present results, we would like to mention that the MILCA method can also be applied on the Fourier space, in similar way as in e.g. (20). In fact for improving results, the algorithm can be applied with some window both in real and Fourier space. Also, we would like to compare the results when using patches over all sky and when applied directly to the all sky.

For the extreme case where $n_c = n_s$, our technique converges to the same solution that the one obtained by a maximum likelihood method (see Eq.(41) for $\hat{\mathbf{f}} = \mathbf{A}$ and $n_c = n_s \leq n_t$). In this case, we can no longer constrain the \mathbf{w} matrix using the minimisation of the variance of components. The last $n_t - n_s$ degrees of freedom are constraint by minimizing the variance of noise, as it is done for the maximum of likelihood method.

$$\hat{\mathbf{S}} = (\mathbf{A}^T \hat{\mathbf{C}}_N^{-1} \mathbf{A})^{-1} \mathbf{A}^T \hat{\mathbf{C}}_N^{-1} \mathbf{T} \quad (41)$$

Acknowledgements

Some of the results in this paper have been derived using the HEALPix package (9).

References

- A.T. Bajkova, A&ApTr 1, 313 (1992).
- Bennett C.L., et al., Astrophysical Journal Letters, 464 (1996) L1.
- Bennett, C.L., et al. 2003, ApJS,148,97 Phys.Rev.D,77,123011 (2003)
- Bertin E., Arnouts S., 1996, A&AS 117, 393 (SExtractor)
- Cardoso, J.-F., Martin, M., Delabrouille, J., Betoule, M., & Patanchon, G. 2008, [arXiv:0803.1814]

- Delabrouille, J., Cardoso, J.-F., & Patanchon, G. 2003, MNRAS, 346, 1089
- Dick, J., Remazeilles, M., & Delabrouille, J. 2009, arXiv:0907.3105v1
- Eriksen, H.K., Banday, A.J., Górski, K.M., & Lilje, P.B. 2004, ApJ, 612, 633
- Eriksen, H. K., Jewell, J. B., Dickinson, C., et al. 2008, ApJ, 676, 10
- Górski, K.M., Hivon, E., Banday, A.J., Wandelt, B.D., Hansen, F.K., Reinecke, M., & Bartelmann, M. 2005, ApJ, 622, 759
- Haslam et al., 1982, A&AS, 47, 1
- Hinshaw G. et al., Astrophysical Journal Supplement, 148 (2003) 63.
- Hinsahw G. et al, Astrophysical Journal Supplement, 180 (2009) 225.
- <http://lambda.gsfc.nasa.gov>
- Larson, D. et al., [arXiv:1001.4635]
- Maino, D., Farusi, A., Baccigalupi, C., et al. 2002, MNRAS, 334, 53
- Hobson, M. P., Jones, A. W., Lasenby, A. N., & Bouchet, F. R. 1998, MNRAS, 300, 1
- Stolyarov, V., Hobson, M. P., Lasenby, A. N., & Barreiro, R. B. 2005, MNRAS, 357, 145
- Remazeilles, M., Delabrouille, J., & Cardoso, J.F. 2010, arXiv:1006.5599
- Schlegel, Finkbeiner & Davis, 1998, ApJ, 500, 525
- Smoot G. F. et al., Astrophysical Journal Supplement, 396 (1992) L13.
- Tegmark, M., de Oliveira-Costa, A., Hamilton, A.J.S., 2003, Phys. Rev. D., 68.123523
- The PLANCK collaboration. **astro-ph/0604069** (2006)
- Vio, R., Andreani, P., 2009 arXiv:0910.4294